Practical Considerations for the Design of Parallel Transmission Pulses at ultra high field

T. Zhao[1], H. Zheng[2], Y-K. Hue[3], T. Ibrahim[2,3], Y. Qian[3], and F. Boada[2,3]

[1]Siemens Medical Solutions, Pittsburgh, Pennsylvania, United States, [2]Bioengineering, University of Pittsburgh, Pittsburgh, Pennsylvania, United States, [3]Radiology, University of Pittsburgh, Pittsburgh, Pennsylvania, United States

Introduction: Parallel transmission was recently proposed as a promising means to accelerate multidimensional selective excitation using multiple coils driven with independent waveforms. Accelerated selective excitation can also reduce specific absorption rate (SAR) and shorten multidimensional RF pulses in such applications as compensation for B_1 and B_0 inhomogeneities. Parallel transmission could be a potential solution for mitigating or solving RF and SAR problems at the ultra high field (e.g, 7T). Many methods have been proposed for designing the RF pulses for multiple coils [1-5]. One of the popular methods was proposed by Grissom *et. al.* [1], which formulated RF pulse design as a quadratic optimization problem in the spatial domain and allowed the use of arbitrary *k*-space trajectories and easy incorporation of B_0 inhomogeneity correction. We applied this method for 7T applications and found that excitation artifacts were generated due to finite gradient raster time. This fact is generally neglected during the implementation of Grissom's method. In this study, two novel methods were proposed to compensate the aforementioned excitation errors and verified using Bloch simulations and phantom experiments on 7T scanner.

Methods: Under the regime of small tip angle, the transverse magnetization produced by any RF pulse waveforms, b(t), from R transmit coils can be approximated by the Fourier integral of an excitation k-space trajectory using the coil's complex B_1 map, s(**x**),

$$m(x) = i\gamma m_0 \sum_{r=1}^{R} s(x) \int_0^T b_r(t) e^{i\mathbf{x}\cdot\mathbf{k}(t)} dt \qquad (1)$$

where γ is the gyromagnetic ratio, m_0 is the equilibrium magnetization magnitude, T is the pulse length, and **k(t)** is defined as the time-reversed integration of the gradient waveforms. As shown in Ref [1], by directly discretizing time to N_t samples and space to N_s samples, we may write:

$$\mathbf{m} = \sum_{r=1}^{R} \mathbf{D}_r \mathbf{A}_r \mathbf{b}_r \qquad (2)$$

where the (i, j)-th element of the matrix A is given in Ref [1] as,

$$a_{ij} = i\gamma m_0 \Delta t e^{i\mathbf{x}_i \bullet \mathbf{k}(t_j)} \qquad (3)$$

For Siemens 7T scanner, the gradient raster time, Δt, is 10 us, which is used as the time step for designing both the spiral trajectory and RF pulses for parallel transmission. However, as shown in the following simulation and experimental results, this direct discretization is not accurate enough due to finite gradient raster time step. To improve to the accuracy, we assumed that the gradient during each Δt period is constant, which leads to a linear k(t) as $k(t\text{-}t_i)=k(t_i)+\{k(t_{i+1})\text{-}k(t_i)\}\times(t\text{-}t_i)/\Delta t$. Since the minimal time step for the RF waveform is 1 us, the RF waveforms within Δt can be specified either as constant or a linear function using more RF sampling data points. The correct a_{ij} can then be obtained by the integration for each Δt period instead of direct discretization as in Ref.1. For **method I**, assuming a constant b(t) within each Δt period, The (i,j)-th element will be

$$a_{ij} = i\gamma m_0 \Delta t e^{i\mathbf{x}_i \bullet \mathbf{k}(t_j)} \times \left(\frac{e^{c_{ij}} - 1}{c_{ij}}\right) \qquad (4)$$

For **method II**, b(t) is assumed to be linear function within each small Δt, that is $b(t\text{-}t_i)=b(t_i)+\{b(t_{i+1})\text{-}b(t_i)\}\times(t\text{-}t_i)/\Delta t$, the (i,j)-th element will be

$$a_{ij} = i\gamma m_0 \Delta t e^{i\mathbf{x}_i \bullet \mathbf{k}(t_j)} \times \left(\frac{e^{c_{ij}} - c_{ij} - 1}{c_{ij}}\right) + i\gamma m_0 \Delta t e^{i\mathbf{x}_i \bullet \mathbf{k}(t_{j-1})} \times \left(\frac{c_{ij-1} e^{c_{ij-1}} - e^{c_{ij-1}} + 1}{c_{ij-1}}\right) \qquad (5)$$

where the correction coefficients c_{ij} is given as,

$$c_{ij} = i\mathbf{x}_i \bullet \{\mathbf{k}(t_{j+1}) - \mathbf{k}(t_j)\} \qquad (6)$$

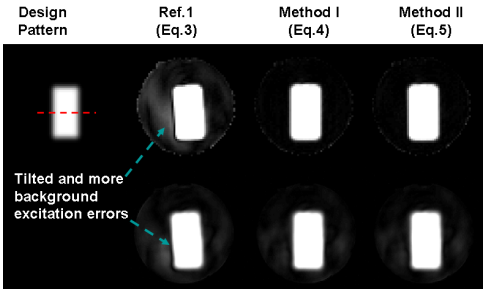

Fig. 1 Comparisons of different RF pulse design methods. Top row, Bloch simulation; Bottom row, phantom experiments.

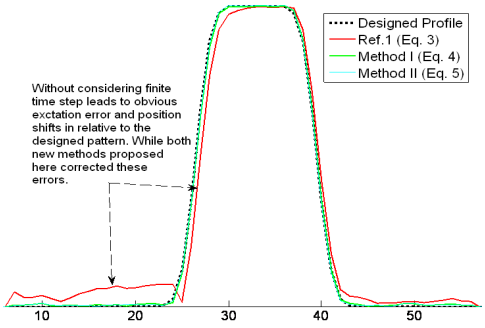

Fig. 2 Excitation profiles along the red dotted line in Fig.1 for different RF pulse design methods

Results and Discussion: All experiments were performed on 7T Siemens scanner equipped with the multi-Tx capabilities. An 8-channel Tx/Rx coil was used and the RF waveforms for each Tx channel can be independently driven. The B_1 map (64×64) for each transmit channel was obtained sequentially with a 2D GRE sequence via varying the excitation voltages from 12.5V to 150V in total 12 steps. The interleaves spiral trajectories were numerical designed with a maximal gradient amplitude, 24 mT/m, slew rate of 80 mT/m/ms, FOV = 200 mm, and matrix size = 32. The acceleration factor for the RF excitation was from 2 to 4, which depends on the number of spiral/EPI interleaves. The design flip angle was 5° and total RF duration was 5.4ms.

Fig.1 shows the comparison of excitation patterns using different RF pulse design methods with acceleration factor of 4. Top row of Fig.1 shows the Bloch simulation results and bottom row of Fig.1 shows the experimental results. It is obvious that the both Bloch simulation and experiments indicate the excitation pattern designed using method described in Ref.1 was tilted slightly to the left and achieved higher residue excitation errors at the background. On the other hand, both **method I** in Eq.4 and **method II** in Eq.5, proposed in this work corrected these excitation errors in the simulations. Fig.2 showed the 1D simulated excitation profiles taken along the red dotted line in Fig.1. The excitation profile using previous method as in Eq.3, showed a slightly shifted excitation profile. To quantify the excitation errors, the mean square errors for the experimental excitation patterns in relative to the designed pattern were determined to be 0.069, 0.0015, and 0.0010 for method in Ref [1], **method I** and **method II**, respectively. The methods described in this study reduced excitation error by more than six times in terms of mean square errors.

Although the tilting was corrected and background errors were smaller using the proposed methods in experiments as shown in the second row of Fig.1, the mean square error reduction factor are only about two, which is much smaller than the simulation results, especial at the background region. We speculated that the excitation errors in the experiments caused by many other factors, such as eddy currents and delays between the RF pulses and gradients. The excitations with other acceleration factors for EP trajectory were also demonstrated (results not shown) and the proposed methods provided better results for both trajectories. When the EP trajectory was used, the excitation without using the correction terms showed obvious ghosting instead of tilting as shown in Fig.1. On the other hand, the experimental results with the use of EP trajectory also showed larger background errors than the simulated results.

Conclusions and Future works: We have proposed two novel methods to correct the excitation artifacts due to finite gradient raster time that was widely neglected. Significant improvement can be observed with the implementation of the proposed methods. However, other factors, such as eddy currents, distorted gradient trajectory are also potential issues to excitation errors and should be carefully compensated during the parallel transmission experiments. Future work will focus on combining the methods in Ref [6] to compensate eddy current induced artifacts.

References: [1] Grissom, W., et al., Magn Reson Med 2006; 56:620. [2]Xu, D., et al., Magn Reson Med 2006; 56:326. [3] Zhu Y., et al., Magn Reson Med 2004; 51:775. [4] Griswold M., et al., Magn Reson Med 2002; 47:1202. [5] Pruessmann KP, et al., Magn Reson Med 1999; 42:952. [6] Zheng H., et al, ISMRM 2010 (#4923)